PHILOSOPHICAL TRANSACTIONS A

rsta.royalsocietypublishing.org

Review

Cite this article: Borrero JC, Lynett PJ, Kalligeris N. 2015 Tsunami currents in ports. *Phil. Trans. R. Soc. A* **373**: 20140372.
http://dx.doi.org/10.1098/rsta.2014.0372

Accepted: 22 July 2015

One contribution of 14 to a theme issue 'Tsunamis: bridging science, engineering and society'.

Subject Areas:
geology, oceanography, civil engineering, ocean engineering

Keywords:
port, tsunami, currents, earthquakes, long waves, seiche

Author for correspondence:
Jose C. Borrero
e-mail: jocabo@jocabo.net

Tsunami currents in ports

Jose C. Borrero[1,2], Patrick J. Lynett[2] and Nikos Kalligeris[2]

[1]eCoast Ltd, Raglan, New Zealand
[2]Department of Civil and Environmental Engineering, University of Southern California, Los Angeles, CA, USA

Tsunami-induced currents present an obvious hazard to maritime activities and ports in particular. The historical record is replete with accounts from ship captains and harbour masters describing their fateful encounters with currents and surges caused by these destructive waves. Despite the well-known hazard, only since the trans-oceanic tsunamis of the early twenty-first century (2004, 2010 and 2011) have coastal and port engineering practitioners begun to develop port-specific warning and response products that accurately assess the effects of tsunami-induced currents in addition to overland flooding and inundation. The hazard from strong currents induced by far-field tsunami remains an underappreciated risk in the port and maritime community. In this paper, we will discuss the history of tsunami current observations in ports, look into the current state of the art in port tsunami hazard assessment and discuss future research trends.

1. Introduction

The Japanese compound word itself ('harbour/port' and 'wave' 津波, tsunami) implies a long-standing and intuitively understood recognition of the vulnerability of port and maritime assets to tsunamis. Indeed, historical accounts provide us with many harrowingly descriptive reports of tsunami effects in ports and on ships at anchor. However, most of these accounts are from the near field and may skew our appreciation for what constitutes a hazardous situation in terms of tsunami effect on ships and or maritime facilities. The line of research discussed here has been motivated due to the fact that tsunami damage is not exclusively caused by surges that result in coastal inundation. Often maritime facilities are vulnerable to tsunami-induced effects not accompanied by flood inducing water levels and which occur many hours after the initial tsunami arrival.

THE ROYAL SOCIETY PUBLISHING

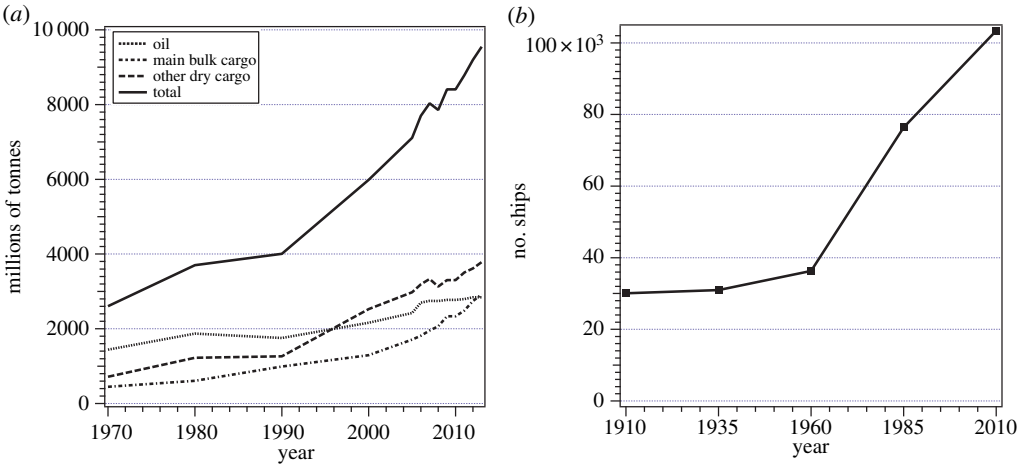

Figure 1. Growth in global ocean cargo tonnage since 1970 (*a*) and global fleet size since 1910 (*b*).

While this phenomenon has been observed repeatedly in the past, it has not been well studied in the context of hazard mitigation. This can be explained by the fact that resolving tsunami current speeds with a numerical model is computationally intensive and requires relatively fine computational mesh sizes resulting in very large numerical grids that require extremely long run times, making them impractical for many modelling efforts. Furthermore, while there are several estimates of current speed based on eyewitness accounts, there is a paucity of quantitative instrumental data on tsunami-induced current speeds making model calibration and validation difficult. Also, recent studies (e.g. [1]) suggest that eyewitness estimates are generally unreliable and tend to overestimate actual current speeds. In recent years, the effects of tsunami currents in ports and harbours have been observed and recorded at many locations around the world.

2. Growth of the maritime sector

Since World War II, the amount of goods and material shipped globally by sea has grown tremendously (figure 1). This is due to several factors, among them population growth, globalization and the shifting of manufacturing centres to Asia. One important factor allowing for this shift has been the advent of the shipping container. The simple technological shift of moving freight in standard-sized containers revolutionized the shipping industry [2], providing cost savings by allowing for goods to be shipped over multiple modes of transport (ship, rail and truck) without additional handling. This reduces direct port costs such as storage and labour as well as indirect costs [3]. Since 1910, the number of cargo ships has grown by nearly three and a half times from just over 30 000 to nearly 104 000 [4]. Besides the growth in shipping, there has also been tremendous growth, particularly in the USA, of private boat ownership and the numbers of marinas needed to satisfy the space requirements for on-the-water storage of these vessels. This growth in ocean cargo, shipping traffic, port capacity and recreational users has significantly increased the exposure of these economic sectors to tsunami hazards. Especially when one considers that prior to 2004, a major trans-oceanic, basin wide tsunami had not occurred since 1964.

3. Historic examples

One of the earliest historical examples of a trans-oceanic tsunami causing damage to ports in the near and far field is that of the great earthquake and tsunami of 13 August 1868 near Arica, Peru (now Chile). In Arica, an American side-wheel gunboat, the USS Wateree, was at anchor when the earthquake struck at 17.05 that afternoon. Commander James H. Gillis reported [5]

Figure 2. In 1868, the USS Wateree was at anchor along with several other ships near the location of the present-day port (*a*). The tsunami waves and surges pushed the ship aground on the beach some 5 km to the north (red dot). The grounded Wateree in 1869 (*b*) and what remains today (*c*). Image credit: Google Earth (*a*), US Naval Historical Centre, Murray Greene Day (*b*) and Jose C. Borrero (*c*).

witnessing the complete destruction of the town of Arica from the deck of the Wateree. By 17.20 the sea was receding and by 17.32 the first tsunami surge was affecting the ships at anchor. Gillis then reported a tremendous current pulling the ship north and east towards shore. As this surge retreated, two smaller ships nearby were left grounded and 90 fathoms (165 m) of anchor chain were paid out from the Wateree as she was pulled seaward. After only a few minutes, a second surge commenced and this time 100 fathoms (183 m) of anchor chain were let out to keep the Wateree under control. Several smaller surges were reported before a third surge occurred between 18.00 and 19.00. As this surge receded, the anchor chain was ripped from the Wateree and the ship was set adrift. The fourth and subsequent surges pushed the Wateree some 5 km north of her initial position where she was eventually grounded at a distance of 430 m inland and 3.7 m above the high water mark. All told, only two members of the Wateree crew were killed; however more than 212 men from the 16 ships at anchor in Arica were lost that day [6]. The Wateree was never recovered and to this day its rusting boilers sit stranded in the desert, a vivid reminder of the terrible tsunami (figure 2).

Sixteen hours later, across the Pacific Ocean, the Arica tsunami arrived in the predawn hours of 15 August in Lyttelton Harbour, on the east coast of New Zealand's South Island. According to Gibson [7], the initial withdrawal induced a current of 12 knots (approx. 6.2 m s^{-1}) and left

areas dry that are normally more than 4.5 m deep at low water. Since the receding water left several ships lying aground they were entirely vulnerable to the returning surge which caused a sea-level rise of more than 7.6 m in approximately 20 min. Newspaper accounts from the time suggest that vessels in Lyttelton Harbour suffered serious damage where ships were torn from their moorings or driven into the wharves. According to the Lyttelton Times of 17 August 1868 (as quoted by Lost Christchurch [8]), the incoming wave:

> was surging round the vessels, tearing them from the different wharfs, and breaking their warps like twine. It caught the John Knox, barque, and dashed her against the screw-pile-jetty, carrying away her starboard quarter, and snapping her best bower cable, also the 8-inch hawsers which held her to the wharf.
>
> The ketch Margaret, lying on the beach near the Government wharf, had her warps carried away, and on the rebound of the wave she was carried into the harbour, where she fouled the schooner Annie Brown, carrying away her own bulwarks, staunchions, and mainmast, and also doing some damage to the schooner. The schooner Jeannie Duncan was lying at the railway wharf alongside the p. s. Novelty. The former has sustained considerable damage, and the Novelty had her bulwarks and staunchions from the fore to the main rigging destroyed. The drawback out of the harbour took the Novelty down as far as Gollan's Bay where she tried to bring up, but her best bower anchor and chain snapped; by this time, however, she had steam up, and was able to steam against it.

Modern reconstruction of the 1868 tsunami at Lyttelton [9] shows that the largest surges occurred during the falling tide, which may have tempered its effects. It also suggests such an event occurring today would result in near total inundation of the Lyttelton Port facilities, potentially crippling one of New Zealand most important ports.

One year earlier, a large earthquake in the Lesser Antilles caused extreme damage in many Caribbean ports [10]. In the Port of Saint Thomas, the commander of the USS Susquehanna noted the formation of a large whirlpool in the centre of the bay, pulling floating debris towards it. The Susquehanna dropped her second anchor holding her in place, enabling the crew to assist with the rescue of stranded and damaged vessels. Another nearby US vessel, the DeSoto, was spun around repeatedly in the receding waves, until finally settling in a large gyre in the centre of bay, spinning slowly for hours. This account is noteworthy in its description of the large eddies and whirlpools that are often generated in ports and harbours during a tsunami, and how these features lead to strong, dynamic and persistent currents.

4. Events in the modern era: 1960, 1964, 2004, 2010 and 2011

The tsunami of 1960 generated in southern Chile can be considered the first significant trans-oceanic tsunami in the era of modern port infrastructure and logistics. Sievers *et al.* [11] vividly relate numerous eyewitness accounts as tsunami waves heavily damaged or destroyed open coast ports such as Ancud, Maullin and Corral in the near field. Notable accounts include quick thinking by crewmen and dock workers at Caleta Mansa, who were working to unload cargo when tsunami effects began. The ship's cables were cut leaving stevedores aboard the ship while others on the dock and on land ran to nearby high ground. Because of the rapidity with which this was done no lives were lost. The ship succeeded in leaving the port even after running aground. The following day, the conditions at Caleta Mansa were sufficiently normal to permit the ships to enter and disembark the stevedores.

At Puerto Corral, several ships were lost including the cargo steamer Carlos Haverbeck (figure 3) which, despite having an anchor over the side and engines running at full power, was dragged into the bay by the flooding tsunami currents. The currents then forced the Carlos Haverbeck into a collision with another ship and over a buoy whose lines became fouled in its propellers. An attempt to secure the ship with the aid of a nearby tug failed as forceful withdrawal of the tsunami surge overcame the Haverbeck's last remaining anchor line and dragged her out

Figure 3. The cargo steamer Carlos Haverbeck sunk in Bahia Corral after being battered by surges from the 1960 Chile Tsunami. (Photo: NOAA/NGDC, Pierre St. Amand.)

towards the open ocean where she ran aground and was stuck until a second wave entered Corral Bay. This surge then carried the Haverbeck towards the centre of the bay grounding her on a large sand bank over which she was dragged several times before finally coming to rest. After the first three largest surges abated, the crew of the Haverbeck had the opportunity to evacuate the ship on the last remaining tender, transporting 10–12 crewmen at a time to safety. As the last load of survivors were in the process of evacuating at 22.40 (approx. 7 h after the earthquake), a strong current developed that smashed the rescue boat against the Haverback's hull, forcing them to make their escape on a small raft. This last group, which included the captain and senior officers, was carried around the bay by the currents until finally running aground at 1.15 on 23rd May, 10 h after the ordeal began.

The effects of the 1960 Chile tsunami were felt in ports across the Pacific, including New Zealand, California, Hawai'i and other Pacific islands, and Japan. In New Zealand, ports along the east coast of the North and South Islands were strongly affected by surges lasting for days. The strongest effects included grounded ships, boat collisions, strong currents and sedimentation and erosion occurring in Whitianga, Gisborne and Lyttelton Harbour [12–14]. In the Hawai'ian Islands, Eaton *et al*. [15] and Cox & Mink [16] reported on the extensive damage to Hilo harbour on Hawai'i and flooding at Kahului harbour on Maui. In California at the Port of Los Angeles, the tsunami caused $1 million in damage with wave heights estimated to be near 2 m and currents estimated to be eight knots (4 m s^{-1}) in the harbour. Over 800 vessels broke their moorings, mostly small craft; 40 were sunk and 200 damaged [17].

In Japan, Susaki Port on Shikoku Island suffered damage as overtopping surges flooded a timber storage facility, turning the timbers into floating debris that damaged many structures [18]. Horikawa [19] reported on the effects of the 1960 tsunami in Japan. He noted the difference between the effects caused by the 1960 tsunami relative to historical near-field events and related this discrepancy to whether or not a particular location was affected by resonance due to a match between the period of the incident tsunami and the fundamental period of the bay or harbour in question. Horikawa also reported on strong current and scour caused by the Chile tsunami in Japan. For example at Hachinoe, a current of 10 knots (approx. 5.1 m s^{-1}) broke moorings, while at Miyako currents of five to eight knots (approx. 2.6–4.1 m s^{-1}) impeded vessel traffic.

Other effects in Japan described by Horikawa [19] include scour around coastal structures leading to collapse.

The great Prince William Sound earthquake of 27 March 1964 [20] generated an extreme tsunami in the near field with run-up in excess of 30 m at several sites and a maximum run-up of 67.1 m in Valdez [21]. The strongest effects outside of Alaska were focused primarily on northern California where the port at Crescent City was destroyed and the town water front was heavily damaged by tsunami run-up of nearly 5 m. However, owing to the location and orientation of the earthquake, the effects in the rest of the Pacific were relatively benign with only Hawai'i reporting significant effects [21].

More than 40 years had passed when the world was again affected by a major trans-oceanic tsunami. Overall, the 26 December 2004 tsunami had a relatively modest impact on ports and shipping in the Indian Ocean although maritime facilities in the near and mid-field (i.e. Indonesia and Thailand) suffered tremendously. Notable were the extreme devastation of the port facilities at Lhok Nga, near Banda Aceh, where the freighter Andalas was capsized at her moorings and a 90 m coal barge was deposited on the beach [22]. Also destroyed was Banda Aceh's principal port facility at Ulee Lheue where a large area of the working water front suffered co-seismic subsidence and large-scale scour and erosion by over washing tsunami flow depths of approximately 10 m [22]. Remarkably neither a pile supported ferry wharf nor mooring dolphins for a power barge at Ulee Lheue were significantly damaged by the tsunami [18] despite the fact that the barge itself was deposited 4 km inland in a residential area. Fritz *et al.* [23] deduced tsunami flow speeds of 2–4 m s^{-1} at inland sites by using particle tracking and image processing of videos shot in the streets of Banda Aceh, several kilometres from the shoreline.

Sheth *et al.* [24] reported that no major ports in mainland India were significantly damaged. However, many intermediate and minor ports were strongly affected. In Kerala in the southwest, several smaller ports were affected by sand deposition reducing the available draft for vessels. In Tamil Nadu, the fishing port at Chennai suffered serious damage resulting in the deaths of 150 fishermen. At the Chennai commercial port, damage was not significant; however, the tsunami broke the mooring lines of one ship allowing it to collide with two others, causing damage to the ships and mooring dolphins. Tsunami-induced sedimentation in the port of Chennai reportedly requires $2.5 million in dredging costs [25]. Elsewhere in the Tamil Nadu region, Maheshwari *et al.* [26] also describe heavy damage at Nagappattinam Port, which remained closed for several weeks after the tsunami. Severe damage was also reported at Kanyakumari Port but no damage was reported at Tuticorin, an important port serving the oil and coal industries.

In the far-field, during the 2004 Indian Ocean tsunami, three occurrences of ships being torn from their moorings were detailed in field survey reports by Okal *et al.* [27–29]. A 50 m freighter was torn from its moorings by strong currents that peaked approximately 6 h after tsunami arrival at Toamasina, Madagascar. Strong currents occurring 4 h after tsunami arrival at Le Port, Reunion Island broke the mooring lines of a 196 m freighter and caused the ship to collide with nearby docks, damaging gantry cranes. And, thirdly, a 285 m freighter whose mooring lines were broken 90 min after tsunami arrival in Salalah, Oman drifted before being intentionally grounded. Another freighter (292 m) was affected by tsunami currents outside the harbour, colliding with a breakwater and incurring minor damage to the fuel tank.

In November 2006, Crescent City, CA, USA suffered the effects of tsunami currents following an M 8.3 earthquake, with the epicentre located near the Kuril Islands [30]. While tsunami warnings were initially cancelled throughout the Pacific due to relatively small wave heights on near-source tide gauges, continued monitoring suggested that the tsunami could be potentially damaging on the US west coast, prompting the issuance of a site-specific advisory for Crescent City. The tsunami peaked in Crescent City approximately 3 h after arrival with a maximum tsunami height of 1.8 m. While the tsunami did not cause any flooding, the strong currents pinned floating docks to their pilings, allowing the water to overtop and causing significant damage, particularly to docks located nearest to the entrance of the inner harbour, where the currents were strongest. The small-boat harbour, which had been severely damaged during the 1964 Alaska tsunami, was re-built in the early 1970s [30]. The ageing docks and the inadequate piling height

(without a cap at the end) allowed some floating docks to be lifted off the pilings, also contributing to the damage.

Ports around the Pacific were affected by the trans-oceanic tsunamis of 2010 and 2011. The Maule, Chile earthquake and tsunami of February 2010 generated strong and damaging currents in San Diego, Ventura and Santa Cruz harbours. Effects included boats swamped by standing waves resulting from the interaction between the ebbing tsunami current and incoming swells, docks damaged by strong currents, boaters forced to stay offshore for over 6 h until the tsunami surges abated, and the breaking free of two large vessels, causing minor damage in collisions with other boats and harbour structures [31].

The Tohoku tsunami of March 2011 disrupted maritime activities throughout the Pacific Ocean. In the near field, port damage was severe throughout the coastline adjacent to the source region, with many ports and marine facilities completely destroyed. Tsunami current speeds of 3–10 m s^{-1} at different stages in the tsunami wave train in Kesennuma Bay were deduced from the analysis of survivor videos by Fritz *et al.* [32], who also showed that the current was the strongest during the latter stages of the outflow phase of the initial wave. The strongest far-field effects and most severe damage occurred in Crescent City. Very strong currents in the inner harbour resulted in severe damage to docks and to boats that remained in the harbour [1]. Fortunately, most of the commercial fishing vessels evacuated the harbour before the tsunami arrived and were spared. In Santa Cruz, strong currents, greater than 13 knots (7 m s^{-1}), accompanied surges that penetrated deep into the rectangular harbour basin, the largest of which occurred some 3 h after initial tsunami arrival, causing considerable damage throughout the harbour. At both Crescent City and Santa Cruz significant sedimentation and scour were also reported [33]. In Ventura, it is worth noting that the strongest and most damaging surges occurred at 01.00 PST on 12 March some 15 h after initial tsunami arrival [31]. Additionally, disruptions to maritime activities and damage by tsunami currents were reported in New Zealand [34] and along the east coast of Australia [35] where tsunami waves affected port facilities for up to 2 days. As noted by Borrero & Greer [14], the effects of the 2011 Tohoku tsunami in California are analogous to tsunamis from South America affecting New Zealand with the orientation and distance between the Japan subduction zone relative to California being roughly similar to the location and orientation of the South American subduction zone to New Zealand. However, the 1960 event notwithstanding, New Zealand last suffered the effects of a major South American tsunami in the late 1800s, when New Zealand's port infrastructure was much less developed than today.

Japan's economy and ability to trade suffered as a result of the extreme level of damage to maritime facilities and ships as a result of the 2011 Tohoku tsunami. The tsunami reportedly caused the loss of as many as 1 million shipping containers forcing carriers to react by extending the life of older containers and by deploying ships to reposition empties [36]. Preliminary estimates indicated that the value of damage to building and infrastructure is about $300 billion while estimates by the World Bank put the cost of the damage caused by the earthquake and tsunami to Japan's economy at $122–$235 billion—equivalent to 2.5–4% of the country's GDP in 2010 [36]. The potential effect on trade even prompted hearings and reports before the US Congress [37,38].

5. History of tsunami hazard mitigation efforts in modern ports

Raichlen [39] described the spectral characteristics of tide gauge records from the 1960 Chile and 1964 Alaska tsunamis at several locations on the North American west coast and two Pacific islands. For the 1964 Alaska event, he found that the spectral responses at three California sites (Santa Monica, Los Angeles and La Jolla) were roughly similar. He also showed that, at Los Angeles, these peaks were also evident during the 1960 Chile tsunami. Besides the low-frequency component ubiquitous to these sites for both events, he noted that the higher frequency components at each site were most probably dependent on the geometric specifics of that particular location.

The work of Camfield [40] summarized what was then the state of the art in models and tools for assessing tsunami hazards in ports and harbours, including discussions on calculating resonant characteristics of irregularly shaped harbour basins (e.g. [41]) and discussion of tsunami wave interaction with coastal structures and tsunami induced currents. Observations of effects in ports from the 2004 Indian Ocean event were used as the backbone for the PIANC [18] document which provided a comprehensive discussion of tsunami basics and port-specific effects. Tsunami data collected on tide gauges throughout the Indian Ocean from the 2004 event were rigorously examined by Rabinovich & Thomson [42], setting the standard for the examination of deep ocean and coastal tide gauge data and the effect of tsunami excitation on harbour or port resonances.

Lynett *et al.* [43] focus on the generation and significance of tsunami-induced jets and eddies in harbours. They discussed a number of recent observations of tsunami 'whirlpools', and a Boussinesq-type model provided good qualitative agreement with the observations. One of the primary conclusions of this paper was that numerical dissipation errors, often due to up-wind discretization of nonlinear advection terms, can greatly influence the generation and evolution of tsunami eddies.

With some confidence in a numerical model's ability to accurately predict tsunami currents in a harbour, it is then feasible to generate current-based hazard maps. Lynett *et al.* [44] summarize recent harbour hazard mapping efforts in California. In this paper, a simple correlation was found between hindcasted (modelled) currents and observed damage. Damage to harbour assets, such as floating docks and vessels, initiates with simulated currents of three knots (approx. $1.5\,\mathrm{m\,s^{-1}}$), and reaches moderate and major damage thresholds at current speeds of six knots and nine knots (approx. 3.1 and $4.6\,\mathrm{m\,s^{-1}}$), respectively. These thresholds are subjected to many uncertainties affecting both the engineering capacity of the infrastructure as well as the tsunami-induced currents themselves. For example, the capacity of a structural component, or the load it can withstand before failing, is highly dependent on its age and deterioration. Predictions of currents are particularly sensitive to bathymetry data errors and to numerical errors (e.g. [43]). However, the current thresholds of 3/6/9 knots noted above are, on average, good indicators of various damage levels. This current–damage connection allows for the generation of damage potential maps, which can be used for both during-event positioning of vessels as well as long-term planning of harbour infrastructure. Indeed, the work of Lynett *et al.* [44] is leading to the development of US national guidelines for maritime tsunami hazard assessment and products by the National Tsunami Hazard Mitigation Program. Outside of the USA, this approach was used by Borrero *et al.* [45] to assess the tsunami hazard at ports in New Zealand.

The relationship between current speed, tsunami height and vessel damage was explored in detail by Suppasri *et al.* [46], who developed detailed loss functions for small vessels using data from more than 20 000 small vessels damaged during the 2011 Tohoku tsunami. Their analysis determined loss functions for both measured tsunami heights and modelled hindcast current speed. They also differentiated the loss functions for sites in the near- and mid-field relative to the tsunami source. However, their velocity estimates relied on a model subject to the numerical dissipation errors described by Lynett *et al.* [43].

6. Present research directions

Predicting the behaviour of tsunami-induced currents in ports and harbours requires an understanding of how these fast-moving flows interact with coastal infrastructure, such as breakwaters and wharves (figure 4). While the strongest average currents are likely to be associated with the resonance modes of a particular harbour [47–50], localized currents may not be. Such localized currents can be driven by boundary effects, jets and large eddies, and so can be de-coupled from the forcing, and possibly resonant, conditions. As flows accelerate around port structures, boundary shear leads to flow separation which, as the oscillatory waves pass, can create transitional turbulent structures, known as coherent eddies or turbulent coherent structures (TCS). These TCS can greatly increase the drag force on affected infrastructure and the ability of the flow to transport debris and floating objects. Large TCS are ubiquitous with tsunamis and their

Figure 4. Counter-rotating TCS offshore of Iwaki city, Fukushima Prefecture, Japan during the 2011 tsunami. (Photo: Reuters/Yomiyuri.)

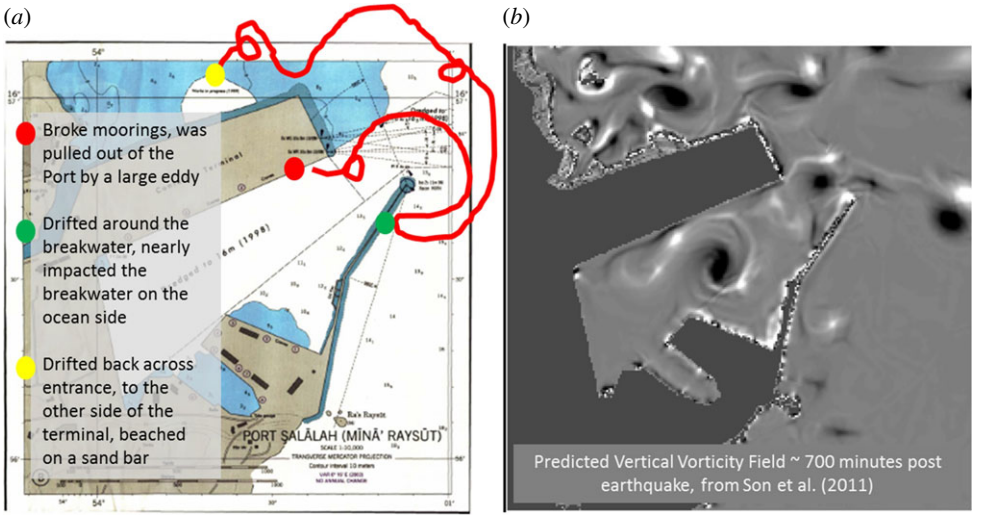

Figure 5. Overview of the tsunami effects in the Port of Salalah, Oman during the 2004 tsunami. (*a*) The path of a 285 m container ship, which drifted on the currents in the port for hours after its mooring lines were broken. (*b*) The numerical recreation of the event, showing the vertical vorticity field; these are the TCS commonly observed in ports during tsunami events. (Online version in colour.)

energetic near shore flows and are more commonly called whirlpools; many of the observations described above note these features. However, as given by Lynett *et al*. [43], the term whirlpool most commonly describes a horizontal eddy with a strong downdraft in the centre (i.e. the drain analogy). The physics of the TCS observed in ports during tsunamis are quite different, and thus the descriptor whirlpool is not physically proper, in much the same way that the term tidal wave is not a good physical descriptor of a tsunami.

As described above, during the 2004 tsunami in the Port of Salalah, Oman, about 90 min after tsunami arrival, extreme currents pulled a 285 m container vessel away from the wharf, breaking all its mooring lines [27]. The vessel then drifted on the currents for hours, spinning three times,

before beaching on a nearby sandbar (figure 5). Significant scour and deposition in the harbour was also noted. Numerical recreation of the event by Son *et al.* [51] indicates that the currents were highly rotational and rapid, but that the tsunami amplitude just outside of the harbour was relatively small, of the order of 40 cm. A question we are left with is: How can such a relatively small tsunami, one that would be considered a common occurrence in tsunami-prone areas, have the potential for such tremendous fluid forces and bottom scour? While the answer to this must necessarily involve aspects such as resonance and wave train properties, it is clear that coherent turbulence structures must play a significant role.

Fundamental research into the generation and evolution of tsunami-induced TCS is essentially non-existent. It would be reasonable to state that the tsunami research community has only recently refined the ability to provide accurate inundation and run-up maps [52] and that more complex physical attributes, such as the second-order dispersion corrections [53–56] and turbulence-driven phenomena (e.g. [51,57]), have not yet been addressed in a widespread or consistent manner. For research into the TCS as related to the near shore tsunami processes discussed here, one must go to the hydraulics community, and specifically to those studying tidal or long wave processes. In this sense, we can consider the whirlpool-like TCS as being 'shallow', and thus possibly exhibiting only weak variability in the vertical direction; similar to the way in which we describe shallow water waves as two-dimensional. Two-dimensional coherent structures are characterized has having a lateral width much greater that the flow depth [58]. In general, the flow is described as being uniform with depth given the large difference in the horizontal and vertical length scales. Shallow water coherent structures are most likely to develop in the presence of strong transverse shear due to fluid flowing past abrupt changes in the bathymetry [59]. Relevant to tsunami processes, the rotation of the structures can be stronger when the shear is created by an unsteady flow as compared to a steady flow [60,61].

While shallow coherent structures might be reasonably described as two-dimensional flow in a mean sense (filtered or averaged across a horizontal length of the order of the local depth), understanding the three-dimensional flow in these coherent structures is necessary to explain the flow persistence and increased mixing known to occur when they are present (e.g. [62,63]). Lin *et al*. [64] provide one of the more detailed descriptions of flow inside shallow TCS using small-scale experimental techniques. They identified areas of increased vorticity (vortex rings) over the water depth within the shallow water structures. The vortex rings cause the flow field to be characterized by a large amount of three-dimensional turbulence. While certain aspects of shallow, whirlpool-like eddy may be described as two-dimensional, it is also clear that the three-dimensionality can be locally very important.

In the past decade, there have been a number of other experimental studies looking at turbulent structures in shallow flows. These studies generally focus on the wakes generated by steady, horizontally uniform flow past an obstacle [65,66], mixing across a horizontal shear layer (e.g. [67]), or slowly varying tidal-like flow through a flow constriction (e.g. [68]). Measurement approaches include a combination of particle image velocimetry techniques to measure the surface velocity field (e.g. [69]) and passive tracer detection to quantify mixing and transport (e.g. [70,71]). A recent study by Jirka & Seol [72] examined an isolated shallow vortex. This configuration is perhaps the most relevant to the tsunami case, where it is likely that the turbulent structures will drift away from the generation area, into otherwise near-uniform flow. Jirka & Seol [72] discussed the importance of bottom friction during the dissipation phase of the rotational structure, and noted that 'laboratory experimentation must be performed at a sufficiently large scale to capture a Reynolds-invariant regime'. They concluded that the variable bottom drag coefficient found in low *Re* (and most experimental) flows produces different 'spin-down' behaviour than would be expected in a high *Re*, geophysical scale flow.

7. Physical modelling of complex tsunami currents in ports

The need to better understand the hydrodynamics of tsunami-induced current dynamics led to a research initiative whose primary goal is to study the complete hydrodynamic structure

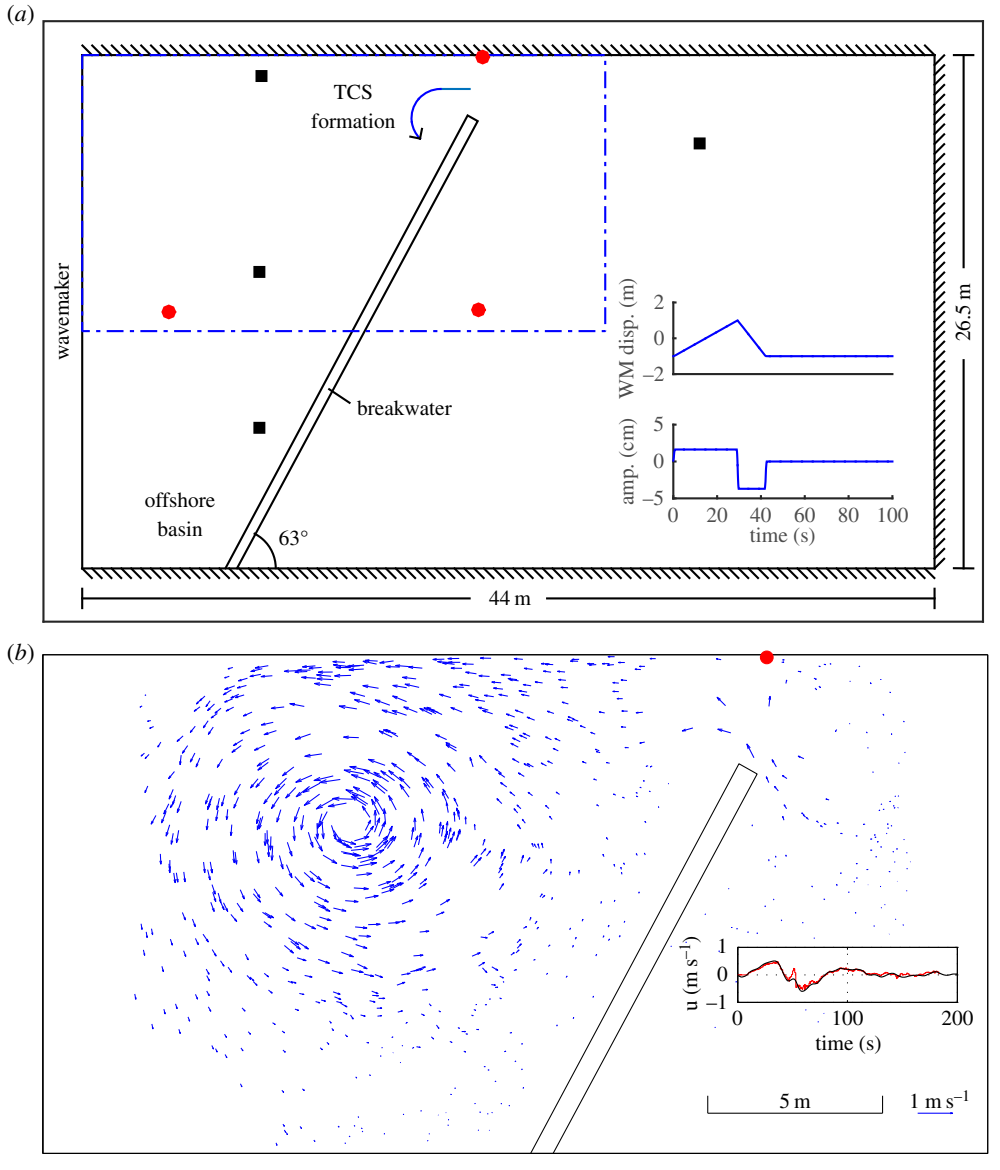

Figure 6. (*a*) The experimental set-up. Dots denote acoustic Doppler velocimetry (ADV) instrument locations, squares denote the location of the overhead HD cameras and the dashed polygon denotes the area of the basin shown in (*b*). In the inset, the top plot corresponds to the wavemaker motion and the bottom plot to the corresponding shallow water surface elevation at the face of the wavemaker. (*b*) Surface velocity vectors as obtained by PTV analysis approximately 2.2 min after the initiation of the experiment. Inset shows a comparison between the ADV-measured velocity in the *x*-direction (along the longer dimension of the basin) and the velocity of the nearest tracer. (Online version in colour.)

of a tsunami-induced shallow TCS in an idealized and controlled (laboratory) environment. The experiments took place in late 2014 in the tsunami wave basin of Oregon State University (see figure 6 for details), and we provide a brief overview of the tests here. A breakwater was built across the basin width at an approximate 63° angle, leaving a 3.2 m gap between the breakwater and the sidewall. The basin was filled to a water depth of 0.55 m, which for a typical harbour channel depth of 15 m corresponds to an approximate 1 : 30 scale. Wavemaker boundary conditions were imposed as a single asymmetric leading elevation wave with a steeper trough

(figure 6*a*, inset). The period of the wave translates to a realistic approximately 5 min prototype time scale; the length scales are undistorted. Surface tracers were seeded to the flow and four overhead HD cameras followed their trajectories. The instantaneous velocity field is obtained using particle tracking velocimetry (PTV) analysis [73].

The wavemaker motion was optimized to generate a stable TCS in the offshore side of the basin. The wavemaker first pushes the water through the breakwater–sidewall gap, forming a small clockwise spinning TCS near the tip of the breakwater. The following sudden drawback of the wavemaker drags the water mass back to the offshore side of the basin, with velocities reaching $1\,\mathrm{m\,s^{-1}}$ at the gap. Flow separation at the tip of the breakwater locally introduces vorticity in the flow. It forms a counter-clockwise spinning TCS, which moves away from the breakwater and grows in size. Figure 6*b* shows the velocity vector distribution from the PTV analysis, approximately 2.2 min after the initiation of the experiment. Maximum surface velocity at this stage is approximately $0.6\,\mathrm{m\,s^{-1}}$ and is found in the outer ring of the TCS. The inner ring around the core of the TCS, with a diameter of approximately 1 m has near zero surface velocity and maximum vorticity (approx. $1.6\,\mathrm{s^{-1}}$). In a later stage, the TCS occupies the whole offshore basin and circulation is still visible 40 min after the initiation of the experiment. The experiment was repeated many times to obtain the characteristics of the chaotic nature of turbulent structures. The results from this study aim to add to the understanding of the dynamics and tsunami-induced TCS in a harbour environment. Furthermore, it offers a unique dataset for the tsunami community, to test how well the numerical models are able to reproduce the hydrodynamics of such small-scale turbulent phenomena.

8. Numerical modelling of tsunami impacts in ports and harbours

As tsunamis are shallow water wave phenomena, and so are commonly modelled with two-horizontal-dimension (2HD) equations, most numerical modelling of tsunamis in ports and harbours also uses 2HD theory. This leads to possibly significant physical disconnect between the simulation and the true geophysical processes that occur as a tsunami enters a port; this disconnect is driven by the components of the flow that are shear and turbulence driven, i.e. the TCS described above. Physically, most shallow TCS are generated through strong horizontal gradients of horizontal vorticity; this gradient causes the horizontal vorticity to rotate and spin about a vertical axis forming the whirlpool-like TCS. As 2HD models are generally unable to capture such strong gradients of horizontal vorticity (indeed the vast majority of models in this class have precisely zero horizontal vorticity everywhere), these models must rely on some type of sub-model to approximate this process. Often simulations tackle this with a simple bottom stress model, based on either a Manning's roughness factor or a quadratic friction coefficient. It is plausible that the simple bottom stress model could generate horizontal shear that approximates, in the bulk or averaged sense, the rotation of horizontal vorticity into a shallow TCS. However, this approximation is likely to be highly sensitive to the specification of the stress model and friction coefficient. Furthermore, the bottom stress formulations (and their accepted friction coefficients) found in tsunami models are based on a steady and uniform boundary layer, neither of which is likely to be a good approximation of the flow near a shallow TCS.

Some attempts have been made to include aspects of three-dimensional flow structure in 2HD models. Nadaoka & Yagi [74], and later Hinterberger *et al.* [75], showed that an approximation of three-dimensional turbulence and the associated mixing inside 2HD models, such as the nonlinear shallow water model, could be done with a so-called backscatter model; essentially, a grid-sized random body force controlled by the local bottom stress. Comparisons with both experimental data and large-eddy simulations showed reasonable agreement. Kim & Lynett [57] extended this concept into the dispersive, Boussinesq-type model. They have performed example simulations of the coherent structures that can be generated by a tsunami in the near shore. However, it should not be expected that simulation of internal dynamics of the complex currents found in ports and harbours can be achieved with anything but a three-dimensional model with a turbulence closure and spatial resolution which physically captures boundary layers. On the

scale of even a small harbour, such a three-dimensional simulation is not currently practical. Despite shortcomings in the underlying physics, some 2HD models nevertheless provide a good approximation of tsunami-induced currents in ports and harbours with relatively low computational cost [1,44,45,76,77].

9. Real-time hazard analysis

Depending on the propagation time from source to site, the present state of computing makes it possible to assess a tsunami's impact before it arrives. For any particular tsunami source descriptor, simulations of full trans-oceanic propagation through to detailed modelling of certain target areas can be accomplished in less time than the physical tsunami needs to arrive at that location allowing for site-specific assessments of tsunami heights, inundation and tsunami currents. Efforts to develop real-time tsunami hazards assessment have been greatly enhanced through the advent of the deep ocean tsunameter [78,79] and tools to access, process and analyse the data.

Presently, the only system to routinely provide reliable and detailed real-time estimates of tsunami height, inundation and current speed for sites in the far field is the Community Model Interface for Tsunamis (ComMIT) numerical modelling tool [80]. The ComMIT model interface was developed by the United States government National Oceanic and Atmospheric Administration's National Centre for Tsunami Research following the 26 December 2004 Indian Ocean tsunami as a way to efficiently distribute assessment capabilities among tsunami-prone countries. The backbone of the ComMIT system is a database of pre-computed deep water propagation results for tsunamis generated by unit displacements on fault plane segments positioned along the Earth's subduction zones. The database is used in conjunction with real-time recording of the tsunami waveforms on one or more of the deep ocean tsunameter stations deployed throughout the oceans to fine tune details of the earthquake source mechanism. The resulting trans-oceanic tsunami propagation results stored in the ComMIT database are then used as boundary inputs for a series of nested near shore grids covering a coastline of interest. More recent versions of the tool facilitate access to the information through an interactive Web interface [81]. The underlying hydrodynamic model used in ComMIT is MOST (Method of Splitting Tsunami) [82], a nonlinear shallow water model. Lynett *et al.* [44] have shown that MOST, at high digital elevation model resolution (approx. 10 m cell size), satisfactorily reproduces tsunami-induced currents, while being overly conservative in its maximum current predictions. This tool was recently applied at Lyttelton Harbour, New Zealand following the M_w 8.2 Iquique, Chile earthquake of 1 April 2014 and tsunami [9] enabling port personnel to confidently stand down from 'alert' status and carry on normal port operations. Real-time analyses for current speeds can be a challenge due to long model run time necessitated by high-resolution computational grids. In the Lyttelton example noted above, the modelling was done on 10 m grids in sufficient time to provide a robust threat assessment. In the case of Tauranga Harbour, New Zealand (described below), hindcast model run times for the Tohoku tsunami using ComMIT on a 10 m grid were nearly 9 h—too long for use in real-time analyses. However, changing the grid resolution to 20 m reduced the model run time to 1.25 h with little loss in model accuracy [83], suggesting this approach is feasible for real-time hazard assessments for tsunami currents. We emphasize, however, that the accuracy of the model results for particular grid resolutions and sizes should be assessed on a site-by-site basis.

A key consideration of any tsunami assessment is of course the description of the tsunami source mechanism. Seismically derived estimates of the earthquake magnitude and location can provide source models sufficient for preliminary assessments. The use of measured tsunami wave forms from multiple tsunameters allows for the further refinement of the source mechanism through a rapid inversion process [84] and the effectiveness of this approach was demonstrated the near field by Wei *et al.* [85]. In general, tsunameter-derived source inversions provide more accurate tsunami estimates at far-field locations faster than is possible when relying on seismically

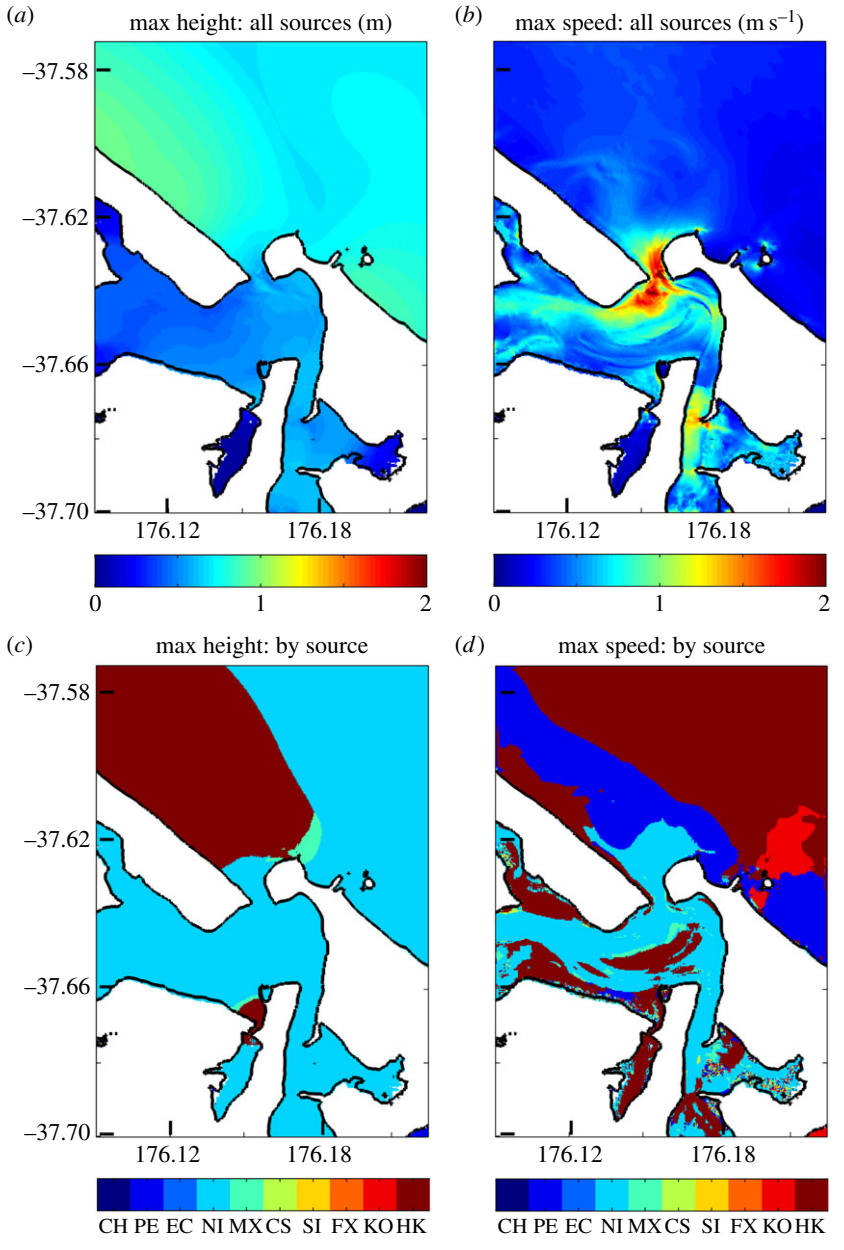

Figure 7. Results from a sensitivity study for Tauranga Harbour, New Zealand showing maximum tsunami height (*a*) and current speed (*b*) for 10 Mw 9.0 earthquakes positioned around the Pacific Rim. Row (*c*,*d*) indicates which source region is responsible for a particular maximum tsunami height (*c*) or current speed (*d*) at that location. Source codes: CH, Chile; PE, Peru; EC, Ecuador; NI, Nicaragua; MX, Mexico; CS, Cascadia; SI, Sitka; FX, Fox Island; KO, Komandorskie; HK, Hokkaido.

or geodetically derived descriptions of the tsunami source, since these methods require hours of processing before results are available [86].

10. Port-specific studies and methodologies

As mentioned above, recent studies in California [44] established methodologies for assessing tsunami current hazards in ports. In New Zealand, Borrero *et al.* [45] systematically extended this analysis to four major ports using the database-driven approach described above. By placing

equivalent tsunami sources at equally spaced azimuthal directions around the Pacific Rim, they conducted a sensitivity analysis of tsunami current hazards as a function of the tsunami source location. The results, as shown in figure 7, suggest that tsunami currents are more sensitive to source location than are tsunami heights. These sorts of assessments can be used to identify locations in ports that are particularly susceptible to strong currents as in Lynett *et al.* [44]. Results from this modelling effort have been integrated into tools for use by emergency managers in New Zealand to provide port-specific warning guidance and information.

11. Conclusion and future directions

In this paper, we have summarized the important aspects of tsunami current hazards in ports and harbours from an engineering and maritime safety standpoint. While tsunami effects on ports can be highly variable depending on the details of the tsunami source, propagation distance and site-specific factors, ports require a detailed and accurate description of the strength, duration and onset of tsunami induced currents in order to properly characterize potential hydrodynamic loads on structures and vessels and follow on effects on port operations and safety. To fully describe these currents, however, requires intensive numerical modelling tools that consider the higher order physics. Nevertheless, some depth-averaged hydrodynamic models are capable of representing tsunami current details to first order, as well as identifying portions of a particular basin most vulnerable to those currents [44]. Further, these models have demonstrated the capacity for these sorts of analyses in real time, allowing for site- and event-specific assessments of an impending tsunami's effects on a particular port. Significant work remains however to integrate these modelling tools into specific action plans for the majority of maritime facilities in tsunami-prone ocean basins. Such a list would include major ports in the South China Sea potentially affected by a tsunami generated on the Manila Trench [87,88] and ports in the Indian Ocean that would be affected by an expected large earthquake on the southern end of the Sumatra subduction zone [89] as well as ports throughout the Pacific and in the Caribbean and Mediterranean Seas. Understanding the hazard presented by tsunami-induced currents in economically important ports allows for hazard planning and mitigation that is driven by exposure and vulnerability. This in turn lowers the long-term risk making the port more cost-efficient to operate and resilient to future tsunami events.

Authors' contributions. J.C.B. organized the manuscript production and composed the historical review, the review of tsunami hazard mitigation in ports and real-time hazard analysis. P.J.L. produced the section on present research directions, directed the physical modelling experiments and wrote on numerical modelling of tsunami currents in ports. N.K. produced the section on the physical modelling of complex tsunami currents which was based on experiments he conducted. All authors gave final approval for publication.

Competing interests. We declare we have no competing interests.

Funding. We received no funding for this study.

References

1. Admire AR, Dengler LA, Crawford GB, Uslu BU, Borrero JC, Greer Sd, Wilson RI. 2014 Observed and modeled currents from the Tohoku-oki, Japan and other recent tsunamis in northern California. *Pure Appl. Geophys.* **171**, 3385–3403. (doi:10.1007/s00024-014-0797-8)
2. Levinson M. 2006 *The box: how the shipping container made the world smaller and the world economy bigger*. Princeton, NJ: Princeton University Press.
3. Hummels DL. 2007 Transportation costs and international trade in the second era of globalization. *J. Econ. Perspect.* **21**, 131–154. (doi:10.1257/jep.21.3.131)
4. Lloyd's Register Fairplay. 2010 *World fleet statistics 1900–2010*. Redhill, UK: Lloyd's Register Fairplay Ltd.

5. Gillis JH. 1868 Reports of USS Powhatan and USS Wateree concerning the earthquake and tidal wave of 13 August 1868 at Arica, Peru. See http://www.history.navy.mil/research/library/online-reading-room/title-list-alphabetically/r/reports-of-arica-peru-earthquake-from-uss-powhatan-and-uss-wateree.html (accessed 28 February 2015).
6. Canque MF. 2007 *Arica 1868, un tsunami y un terremoto*. Coedición Centro de Investigaciones Barros Arana y Universidad de Tarapacá, Arica, Santiago de Chile.
7. Gibson F. 1868 On the wave phenomena observed in Lyttelton Harbour, August 15, 1868. *Trans. Proc. NZ Inst.* **1**, 195–196.
8. Lost Christchurch. 2012 The earthquake wave at Lyttelton, 1868. See http://lostchristchurch.org.nz/the-earthquake-wave-at-lyttelton-1868 (accessed 15 March 2015).
9. Goring JC, Borrero DG. 2015 South American tsunamis in Lyttelton Harbor, New Zealand. *Pure Appl. Geophys.* **172**, 757–772. (doi:10.1007/s00024-014-1026-1)
10. Reid HF, Taber S. 1920 The Virgin Islands earthquakes of 1867–1868. *Bull. Seismol. Soc. Am.* **10**, 9–30.
11. Sievers HA, Villegas GC, Barros G. 1963 The seismic sea wave of 22 May 1960 along the Chilean coast. *Bull. Seismol. Soc. Am.* **53**, 1125–1190.
12. Heath RA. 1976 The response of several New Zealand harbours to the 1960 Chilean tsunami. *Bull. R. Soc. NZ* **15**, 71–82.
13. de Lange WP, Healy TR. 1986 New Zealand tsunamis 1840–1982. *N. Z. J. Geol. Geophys.* **29**, 115–134. (doi:10.1080/00288306.1986.10427527)
14. Borrero JC, Greer SD. 2013 Comparison of the 2010 Chile and 2011 Japan tsunamis in the far field. *Pure Appl. Geophys.* **170**, 1249–1274. (doi:10.1007/s00024-012-0559-4)
15. Eaton JP, Richter DH, Ault WU. 1961 The tsunami of May 23, 1960, on the Island of Hawaii. *Bull. Seismol. Soc. Am.* **51**, 135–157.
16. Cox DC, Mink JF. 1963 The tsunami of 23 May 1960 in the Hawaiian Islands. *Bull. Seismol. Soc. Am.* **53**, 1191–1209.
17. Lander JF, Lockridge PA 1989 *United States tsunamis* (*including United States possessions*) *1690–1988*. Boulder, CO: National Geophysical Data Center, National Oceanic and Atmospheric Administration, Department of Commerce.
18. PIANC. 2009 *Mitigation of tsunami disasters in ports*. Report no. 112. Brussels, Belgium: World Association for Waterborne Transport Infrastructure.
19. Horikawa K. 1961 *Tsunami phenomena in the light of engineering view-point*. Report on the Chilean tsunami of May 24, 1960, as observed along the coast of Japan. Tokyo, Japan: University of Tokyo.
20. Plafker G. 1969 Tectonics of the March 27, 1964 Alaska earthquake. US Geological Survey Professional Paper 543–I.
21. National Geophysical Data Center/World Data Service (NGDC/WDS): Global Historical Tsunami Database. National Geophysical Data Center, NOAA. (doi:10.7289/V5PN93H7) Accessed May 2015.
22. Borrero JC. 2005 Field survey of northern Sumatra and Banda Aceh, Indonesia after the tsunami and earthquake of 26 December 2004. *Seismol. Res. Lett.* **76**, 312–320. (doi:10.1785/gssrl.76.3.312)
23. Fritz HM, Borrero JC, Synolakis CE, Yoo J. 2006 2004 Indian Ocean tsunami flow velocity measurements from survivor videos. *Geophys. Res. Lett.* **33**, L24605. (doi:10.1029/2006GL026784)
24. Sheth A, Sanyal S, Jaiswal A, Gandhi P. 2006 Effects of the December 2004 Indian Ocean tsunami on the Indian mainland. *Earthquake Spectra* **22**, 435–473. (doi:10.1193/1.2208562).
25. United Nations Conference on Trade and Development: UNCTAD. 2005 *Review of maritime transport*, p. 148. United Nations Publication.
26. Maheshwari BK, Sharma ML, Narayan JP. 2005 Structural damages on the coast of Tamil Nadu due to tsunami caused by December 26, 2004 Sumatra earthquake. *ISET J. Earthquake Technol.* **42**, 63–78.
27. Okal EA, Fritz HM, Raad PE, Synolakis CE, Al-Shijbi Y, Al-Saifi M. 2006 Oman field survey after the December 2004 Indian Ocean tsunami. *Earthquake Spectra* **22**, 203–218. (doi:10.1193/1.2202647)
28. Okal EA, Sladen A, Okal EA-S. 2006 Rodrigues, Mauritius and Reunion islands field survey after the December 2004 Indian Ocean tsunami. *Earthquake Spectra* **22**, 241–261. (doi:10.1193/1.2209190)

29. Okal EA, Fritz HM, Raveloson R, Joelson G, Pancockova P, Rambolamanana G. 2006 Madagascar field survey after the December 2004 Indian Ocean tsunami. *Earthquake Spectra* **22**, 263–283. (doi:10.1193/1.2202646)
30. Dengler LA, Uslu B, Barberopoulou A, Borrero JC, Synolakis CE. 2008 The vulnerability of Crescent City, California, to tsunamis generated by earthquakes in the Kuril Islands region of the northwestern Pacific. *Seismol. Res. Lett.* **79**, 608–619. (doi:10.1785/gssrl.79.5.608)
31. Wilson RI *et al*. 2013 Observations and impacts from the 2010 Chilean and 2011 Japanese tsunamis in California (USA). *Pure Appl. Geophys.* **170**, 1127–1147. (doi:10.1007/s00024-012-0527-z)
32. Fritz HM, Phillips DA, Okayasu A, Shimozono T, Liu H, Mohammed F, Skanavis V, Synolakis CE, Takahashi T. 2012 The 2011 Japan tsunami current velocity measurements from survivor videos at Kesennuma Bay using LiDAR. *Geophys. Res. Lett.* **39**, L00G23. (doi:10.1029/2011GL050686)
33. Wilson R, Davenport C, Jaffe BE. 2012 Sediment scour and deposition within harbors in California (USA), caused by the March 11, 2011 Tohoku-oki tsunami. *Sediment. Geol.* **282**, 228–240. (doi:10.1016/j.sedgeo.2012.06.001)
34. Borrero JC, Bell R, Csato C, de Lange WP, Goring D, Greer DS, Pickett V, Power WL. 2013 Observations, effects and real time assessment of the March 11, 2011 Tohoku-oki tsunami in New Zealand. *Pure Appl. Geophys.* **170**, 1229–1248. (doi:10.1007/s00024-012-0492-6)
35. Hinwood JB, McLean EJ. 2012 Effects of the March 2011 Japanese tsunami in bays and estuaries of SE Australia. *Pure Appl. Geophys.* **170**, 1207–1227. (doi:10.1007/s00024-012-0561-x)
36. United Nations Conference on Trade and Development: UNCTAD. 2011 *Review of maritime transport 2011*, p. 233. United Nations Publication.
37. Nanto D, Cooper W, Donnelley J, Johnson R. 2011 Japan's 2011 earthquake and tsunami: economic effects and implications for the United States. Report R41702. Washington, DC: Congressional Research Service.
38. Canis B. 2011 The motor vehicle supply chain: effects of the Japanese earthquake and tsunami. Report R41831. Washington, DC: Congressional Research Service.
39. Raichlen F. 1970 Tsunamis: some laboratory and field observations. Coastal Engineering Proceedings. Retrieved from http://journals.tdl.org/icce/index.php/icce/article/viewArticle/2732.
40. Camfield FE. 1980 Tsunami engineering. US Army Corps of engineers. Coastal Engineering Research Center, Special Report, no. 6.
41. Lee JJ. 1971 Wave induced oscillations in harbours of arbitrary geometry. *J. Fluid Mech.* **45**, 375–394. (doi:10.1017/S0022112071000090)
42. Rabinovich AB, Thomson RE. 2007 The 26 December 2004 Sumatra tsunami: analysis of tide gauge data from the World Ocean Part 1. Indian Ocean and South Africa. *Pure Appl. Geophys.* **164**, 261–308. (doi:10.1007/s00024-006-0164-5)
43. Lynett PJ, Borrero JC, Weiss R, Son S, Greer D, Renteria W. 2012 Observations and modeling of tsunami-induced currents in ports and harbors. *Earth Planet. Sci. Lett.* **327–328**, 68–74. (doi:10.1016/j.epsl.2012.02.002)
44. Lynett PJ, Borrero J, Son S, Wilson R, Miller K. 2014 Assessment of the tsunami-induced current hazard. *Geophys. Res. Lett.* **41**, 2048–2055. (doi:10.1002/2013GL058680)
45. Borrero JC, Goring DG, Greer SD, Power WL. 2014 Far-field tsunami hazard in New Zealand ports. *Pure Appl. Geophys.* **172**, 731–756. (doi:10.1007/s00024-014-0987-4)
46. Suppasri A, Muhari A, Futami T, Imamura F, Shuto N. 2014 Loss functions for small marine vessels based on survey data and numerical simulation of the 2011 Great East Japan tsunami. *J. Waterw. Port Coast Ocean Eng.* **140**, 04014018. (doi:10.1061/(ASCE)WW.1943-5460.0000244)
47. Omori F. 1902 On tsunamis around Japan (in Japanese). *Rep. Imp. Earthquake Comm.* **34**, 5–79.
48. Honda K, Terada T, Yoshida Y, Isitani D. 1908 An investigation on the secondary undulations of oceanic tides. *J. College Sci. Imper. Univ. Tokyo*, 1–110.
49. Raichlen F. 1979 Bay and harbour response to tsunamis. In *Proc. National Science Foundation Workshop on Tsunamis* (eds LS Hwang, YK Lee), pp. 188–221. Pasadena, CA: Tetra Tech.
50. Rabinovich AB. 1997 Spectral analysis of tsunami waves: separation of source and topography effects. *J. Geophys. Res.* **102**, 12 663–12 676. (doi:10.1029/97JC00479)
51. Son S, Lynett JP, Kim D-H. 2011 Nested and multi-physics modeling of tsunami evolution from generation to inundation. *Ocean Modell.* **38**, 96–113. (doi:10.1016/j.ocemod.2011.02.007)
52. Barberopoulou A, Borrero JC, Uslu B, Legg M, Synolakis CE. 2011 A second generation of

tsunami inundation maps for the State of California. *Pure Appl. Geophys.* **168**, 2133–2146. (doi:10.1007/s00024-011-0293-3)
53. Horrillo J, Kowalik Z, Shigihara Y. 2006 Wave dispersion study in the Indian Ocean tsunami of December 26, 2004. *Mar. Geod.* **29**, 149–166. (doi:10.1080/01490410600939140)
54. Grue J, Pelinovsky EN, Fructus D, Talipova T, Kharif C. 2008 Formation of undular bores and solitary waves in the Strait of Malacca caused by the 26 December 2004 Indian Ocean tsunami. *J. Geophys. Res.* **113**, C05008. (doi:10.1029/2007JC004343)
55. Kirby JT, Pophet N, Shi F, Grilli ST. 2009 Basin scale tsunami propagation modeling using Boussinesq models: parallel implementation in spherical coordinates. In *Proc. WCCE–ECCE–TCCE Joint Conf. on Earthquake and Tsunami, Istanbul, Turkey, 22–24 June 2009*, paper 100.
56. Kim D-H, Lynett PJ, Socolofsky SA. 2009 A depth-integrated model for weakly dispersive, turbulent, and rotational fluid flows. *Ocean Modell.* **27**, 198–214. (doi:10.1016/j.ocemod.2009.01.005)
57. Kim D-H, Lynett P. 2011 Turbulent mixing and scalar transport in shallow and wavy flows. *Phys. Fluids* **23**, 016603. (doi:10.1063/1.3531716)
58. Negretti ME, Socolofsky SA, Rummel AC, Jirka GH. 2005 Stabilization of cylinder wakes in shallow water flows by means of roughness elements: an experimental study. *Exp. Fluids* **38**, 403–414. (doi:10.1007/s00348-004-0918-8)
59. Socolofsky SA, Jirka GH. 2004 Large-scale flow structures and stability in shallow flows. *J. Environ. Eng. Sci.* **3**, 451–462. (doi:10.1139/s04-032)
60. Signell RP, Geyer WR. 1991 Transient eddy formation around headlands. *J. Geophys. Res.* **96**, 2561–2575. (doi:10.1029/90JC02029)
61. Geyer WR. 1993 Three-dimensional tidal flow around headlands. *J. Geophys. Res.* **98**, 955–966. (doi:10.1029/92JC02270)
62. Sous DA, Bonneton NB, Sommeria JC. 2004 Turbulent vortex dipoles in a shallow water layer. *Phys. Fluids* **16**, 2886–2898. (doi:10.1063/1.1762912)
63. Cieslik AR, Kamp LPJ, Clercx HJH, van Heijst GJF. 2010 Three-dimensional structures in a shallow flow. *J. Hydro-Environ. Res.* **4**, 89–101. (doi:10.1016/j.jher.2010.04.003)
64. Lin J-C, Ozgoren M, Rockwell D. 2003 Space-time development of the onset of a shallow-water vortex. *J. Fluid Mech.* **485**, 33–66. (doi:10.1017/S0022112003004269)
65. Lloyd PM, Stansby PK. 1997 Shallow water flow around model conical island of small slope II. Submerged. *J. Hydraul. Eng.* **123**, 1068–1077. (doi:10.1061/(ASCE)0733-9429(1997)123:12(1068))
66. Chen D, Jirka G. 1995 Experimental study of plane turbulent wakes in a shallow water layer. *Fluid Dyn. Res.* **16**, 11–41. (doi:10.1016/0169-5983(95)00053-G)
67. Uijttewaal WSJ, Tukker J. 1998 Development of quasi two-dimensional structures in a shallow free-surface mixing layer. *Exp. Fluids* **24**, 192–200. (doi:10.1007/s003480050166)
68. Nicolau del Roure F, Socolofsky SA, Chang K-A. 2009 Structure and evolution of tidal starting jet vorties at idealized barotropic inlets. *J. Geophys. Res.* **114**, C05024. (doi:10.1029/2008JC004997)
69. Weitbrecht V, Kühn G, Jirka GH. 2002 Large scale PIV-measurements at the surface of shallow water flows. *Flow Meas. Instrum.* **13**, 237–245. (doi:10.1016/S0955-5986(02)00059-6)
70. Carmer CF. 2005 Shallow turbulent wake flows: momentum and mass transfer due to large-scale coherent vortical structures. PhD thesis, University of Karlsruhe, Germany.
71. Carmer CFV, Rummel AC, Jirka GH. 2009 Mass transport in shallow turbulent wake flow by planar concentration analysis technique. *J. Hydraul. Eng.* **135**, 257–270. (doi:10.1061/(ASCE)0733-9429(2009)135:4(257))
72. Jirka GH, Seol D-G. 2010 Dynamics of isolated vortices in shallow flows. *J. Hydro-Environ. Res.* **4**, 65–73. (doi:10.1016/j.jher.2010.04.011)
73. Crocker JC, Grier DG. 1996 Methods of digital video microspocy for colloidal studies. *J. Colloid Interface Sci.* **179**, 298–310. (doi:10.1006/jcis.1996.0217)
74. Nadaoka K, Yagi H. 1998 Shallow-water turbulence modeling and horizontal large-eddy computation of river flow. *J. Hydraul. Eng.* **124**, 493–500. (doi:10.1061/(ASCE)0733-9429(1998)124:5(493))
75. Hinterberger C, Frohlich J, Rodi W. 2007 Three-dimensional and depth-averaged large-eddy simulations of some shallow water flows. *J. Hydraul. Eng.* **133**, 857–872. (doi:10.1061/(ASCE)0733-9429(2007)133:8(857))
76. Cheung KF, Bai Y, Yamazaki Y. 2013 Surges around the Hawaiian Islands from the 2011

Tohoku tsunami. *J. Geophys. Res. Oceans* **118**, 5703–5719. (doi:10.1002/jgrc.20413)
77. Arcos EM, LeVeque RJ. 2014 Validating velocities in the GeoClaw tsunami model using observations near Hawaii from the 2011 Tohoku tsunami. *Pure Appl. Geophys.* **172**, 849–867. (doi:10.1007/s00024-014-0980-y)
78. Bernard EN, González FI, Meinig C, Milburn HB. 2001 Early detection and real-time reporting of deep-ocean tsunamis. In *Proc. Int. Tsunami Symp., Seattle, WA, USA, 7–10 August 2001*, paper R-6.
79. Rabinovich AB, Eble MC. In press. Deep-ocean measurements of tsunami waves. *Pure Appl. Geophys*. (doi:10.1007/s00024-015-1058-1)
80. Titov VV, Moore CW, Greenslade DJM, Pattiaratchi C, Badal R, Synolakis CE, Kânoğlu U. 2011 A new tool for inundation modeling: community modeling interface for tsunamis (ComMIT). *Pure Appl. Geophys.* **168**, 2121–2131. (doi:10.1007/s00024-011-0292-4)
81. Kamb L, Moore C, Berger E. 2014 ComMIT and Tweb integration: global tsunami modeling done locally. In *Proc. AGU Fall Meeting, San Francisco, CA, 15–19 December 2014*, abstract S21A-4409. Washington, DC: American Geophysical Union.
82. Titov VV, Synolakis CE. 1998 Numerical modeling of tidal wave runup. *J. Waterw. Port Coast Ocean Eng.* **124**, 157–171. (doi:10.1061/(ASCE)0733-950X(1998)124:4(157))
83. Borrero JC, LeVeque RJ, Greer SD, O'Neill S, Davis BN. 2015 Observations and modelling of tsunami currents at the Port of Tauranga, New Zealand. In *Proc. Australasian Coasts and Ports Conf., Auckland, New Zealand, 15–18 September 2015*.
84. Percival DB, Denbo DW, Eble MC, Gica E, Mofjeld HO, Spillane MC, Tang L, Titov VV. 2010 Extraction of tsunami source coefficients via inversion of DART buoy data. *Nat. Hazards* **58**, 567–590. (doi:10.1007/s11069-010-9688-1)
85. Wei Y, Chamberlin C, Titov VV, Tang L, Bernard EN. 2012 Modeling of the 2011 Japan tsunami: lessons for near-field forecast. *Pure Appl. Geophys.* **170**, 1309–1331. (doi:10.1007/s00024-012-0519-z)
86. Wei Y, Newman AV, Hayes GP, Titov VV, Tang L. 2014 Tsunami forecast by joint inversion of real-time tsunami waveforms and seismic or GPS data: application to the Tohoku 2011 tsunami. *Pure Appl. Geophys.* **171**, 3281–3305. (doi:10.1007/s00024-014-0777-z)
87. Megawati K, Shaw F, Sieh K, Huang Z, Wu T-R, Lin Y, Tan SK, Pan T-C. 2009 Tsunami hazard from the subduction megathrust of the South China Sea: part I. Source characterization and the resulting tsunami. *J. Asian Earth Sci.* **36**, 13–20. (doi:10.1016/j.jseaes.2008.11.012)
88. Okal EA, Synolakis CE, Kalligeris N. 2010 Tsunami simulations for regional sources in the South China and adjoining seas. *Pure Appl. Geophys.* **168**, 1153–1173. (doi:10.1007/s00024-010-0230-x)
89. Sieh K. 2006 Sumatran megathrust earthquakes: from science to saving lives. *Phil. Trans. R. Soc. A* **364**, 1947–1963. (doi:10.1098/rsta.2006.1807)